THE E-HY*D*RID

Georges Vael, Sjoerd Eggenkamp and Peter Achten
Innas BV
Nikkelstraat 15
4823 AE Breda, The Netherlands
Phone ++31 76 5424080, Fax +31 76 5424090
E-mail: gvael@innas.com

ABSTRACT

In earlier research, it has been shown that the hydrid driveline concept, when applied to a standard average family car, reduces fuel consumption and CO_2-emissions with more than 50%, without compromising any of the original vehicle performance characteristics. The hydrid driveline concept is a serial hydraulic hybrid driveline, which can replace the mechanical driveline with only a very limited increase in vehicle cost and weight. The driveline is built around a hydraulic pressure grid, to which a secondary energy source can be easily attached. This presents the obvious opportunity of adding a small electric energy source (battery, e-motor/generator and hydraulic pump/motor), which can be sized to deliver only the average power required in urban driving. The hydraulic accumulators deal with the power peaks, which would otherwise be strongly determining for the size and endurance of the electric system. This paper presents the results of a study into such an e-hydrid vehicle. It shows that for a typical commuter car with hydrid driveline, the addition of an electro-hydraulic system with only a 7 kW e-motor and 8 MJ effective battery capacity results in an all-electric range of 25 km and a very friendly load for the e-motor and the battery.

KEYWORDS: Electrohydraulic hybrid, hydrid, emission free urban driving

1. INTRODUCTION

Modern passenger cars are required to have a high top-speed, fast acceleration and high gradeability. These extreme requirements lead to high installed engine powers and high maximum wheel torques. In every day driving, however, the power and torque demands are far less. In conventional mechanical passenger car drivelines, with their permanent connection between engine and load, this implies that the engine is almost always forced to run in operating points with low power and torque and thus at bad part load efficiencies.

In 2008, Innas BV introduced the 'hy*d*rid', a new hydraulic hybrid driveline concept. When the original hydrid driveline is used in an average passenger car, it realizes a reduction in fuel consumption and CO_2-emissions of around 50%, without compromising the performance and with only a very limited increase in vehicle weight and costs. It does so by using the ICE engine in on/off mode: when the engine is on, it is forced to work in operating points with high efficiencies, supplying energy to a hydraulic accumulator. When the accumulator is full, the engine is switched off and the energy necessary to drive the vehicle is then taken from the accumulator storage. In this way, significant energy losses in the primary part of the driveline are avoided. Obviously, if the vehicle performance is to be kept at the same level, also the secondary part of the driveline has to be laid out for the extreme requirements but will predominantly operate in far more moderate conditions. In order to avoid the efficiency gain at the primary side being largely lost again at the secondary side, it is imperative that the secondary side topology and components allow for part load operation with good efficiency.

As a consequence, conventional hydraulic components, which display rather poor part load efficiencies, are not suited for hybrid drivelines for passenger cars. In the hydrid driveline, bad secondary side part load efficiencies are avoided by the use of the new 'Floating Cup' (FC) axial piston displacement principle for all hydrostatic units and by the use of the Innas Hydraulic Transformer (IHT) in combination with fixed displacement drive units. The hydrid driveline has been described in detail in previous publications (for instance in [1] and [2]) but a brief recapitulation of the background to its performance is given in section 2 of this paper.

On/off operation of the combustion engine and the associated gain in average efficiency can also be realised with an equivalent serial electric hybrid driveline, using electric batteries as intermediate energy storage. This option has distinct disadvantages:

- Electric batteries have a good energy density but a very poor power density. If they have to be laid out to accommodate the total maximal power requirement of an average passenger car in extreme conditions, large and heavy batteries have to be chosen, which are expensive. For this application, the current batteries of choice would be Lithium-Ion batteries, which require expensive control systems to safeguard them when subjected to these high power loads.
- Electro-mechanic drive units have a low power and torque density. Consequently, electro-mechanic drive units that can cope with the extreme requirements are large and heavy and thus expensive.
- Contrary to what is often suggested, the prices of batteries and e-motors may not be expected to drop when automotive series sizes are reached. The resources of the required raw materials (Lithium and rare earth materials like Lanthanum and Neodymium) are limited or heavily controlled. If a significant part of the current fleet of passenger cars is to be equipped with a serial electric drive line, the material shortage will keep the electric component price high. ([3], [4]).
- Global warming is – as the term suggests – a global problem and thus CO_2-emissions are a global issue. The emissions of the current fleet of passenger cars in western countries are the smaller part of the problem. The exponential growth of mobility in countries like India or China is a much bigger threat. In those countries, affordable passenger cars are in great demand and electric hybrid solutions will be too expensive to be an alternative for the customers there.

Instead of using this serial electric hybrid passenger car driveline, which is functionally and performance-wise fully equivalent to the hydrid solution, one could also opt for a large number of other possible electric hybrid solutions, ranging from mild-hybrids, parallel hybrids or combinations of serial and parallel hybrids. These solutions however, are either still very expensive or greatly hampered in their performance by the urge to choose small e-motors and batteries in order to keep the cost down.

Recently, a number of studies (see for instance [5], [6] and [7]) have been published which put question marks to the CO_2 abatement potential of electric hybrid vehicles. In addition to that, car manufacturers seem to have become a lot more critical towards electric hybrid solutions. They are clearly looking for alternative solutions, probably because of a growing awareness of the negative cost and performance consequences that electric hybrid solutions invariably imply.

Of course, CO_2 abatement is not the only reason to strive for electric or electric hybrid passenger cars. Other drivers are the reduction of particulate emissions in urban areas or the realisation that transportation will eventually have to be independent of fossil fuels.

In this context, the hydrid driveline offers a very interesting possibility: as it is built around a hydraulic pressure grid, powered by an ICE-pump combination, it is very easy to add a second, electric energy source. This can be realised with a simple fixed displacement FC-pump, driven by an e-motor, which takes its energy from a battery.

In this e-hydrid driveline, the electric and the hydraulic storage systems can both be used to their own optimal capabilities:

- The electric battery, with its superior energy density but very poor power density, is used to deliver the average low power demand of city driving and to ensure a sufficient emission-free range.
- The hydraulic accumulator, with its superior power density but very poor energy density, is used to cope with the high powers during accelerating and braking.

The resulting passenger car offers the performance and extra-urban range of its conventional counterpart as well as emission-free driving in urban areas.

The paper reports the results of a design, sizing and performance study for such an e-hydrid passenger car. Section 2 introduces the reference vehicle and the layout, sizing and performance of its hydrid variant. Section 3 covers the layout and sizing of the added electric part of the driveline. Section 4 presents simulation results for the e-hydrid on representative cycles. Finally, in section 5, a conclusion and outlook are given.

2. THE REFERENCE VEHICLE AND ITS HYDRID VERSION

2.1. The reference vehicle

Table 1 lists the specifications of the reference vehicle for this study. A typical commuter car was chosen: with enough space for four passengers and their luggage and with very decent performance characteristics.

The data presented are generic but representative for this type of car.

Table 1. Specifications, performance and NEDC figures of the reference vehicle

Specifications			
Engine	Diesel, 80 kW	Load capacity	500 kg
Transmission	Manual, 5 speed	$r_{tyre, dynamic}$	0.31 m
$i_{gearbox}$	3.61/ 1.95 / 1.28 / 0.97 / 0.78	f_{roll}	0.007
$i_{differential}$	3.1	C_D	0.26
Curb weight	1200 kg	$A_{frontal}$	2.5 m2
Performance and CO_2-emission (NEDC)		Fuel Consumption (NEDC)	
Top speed	190 km/h	City	5.8 l/100 km
Acceleration	0–100 km/h in 10 s	Highway	3.8 l/100 km
CO_2-emission	120 gr/km	Combined	4.5 l/100 km

2.2. The hydrid concept

The original hydrid driveline concept is shown in figure 1. It has been described in detail in several earlier publications (see for instance [1] and [2]) Here, only a brief recapitulation of its essential properties is given.

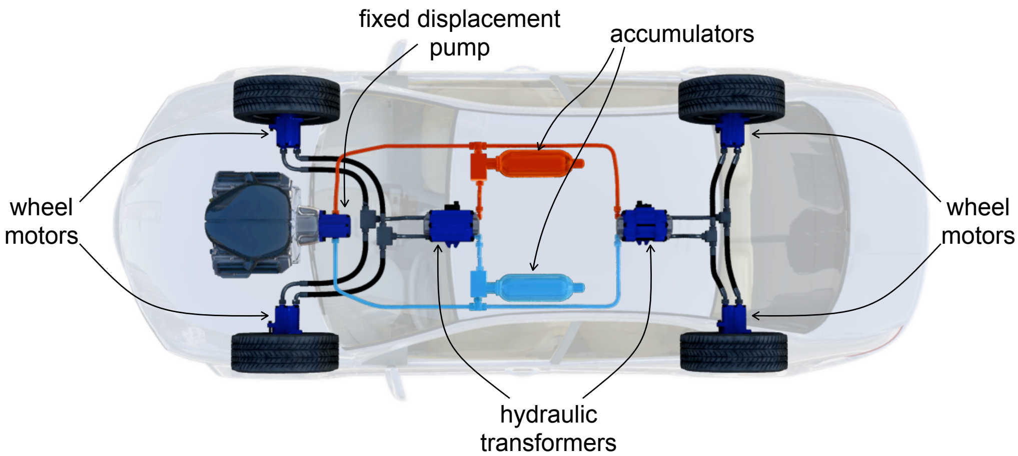

Figure 1. The hydrostatic drive line for the hydrid four-wheel drive.

The hydrid driveline is built around on a hydraulic pressure grid, the Common Pressure Rail (CPR), which consists of a high-pressure line and a low-pressure line. An accumulator is connected to each line.

A fixed displacement pump, directly driven by the ICE, upholds the pressure difference between the two lines of the CPR. When the pressure in the high-pressure line drops below the lowest acceptable level of the accumulator, the ICE is switched on and oil is pumped from the low-pressure line to the high-pressure line. When the pressure reaches the highest acceptable level, the ICE is switched off.

At a 200 to 400 bar pressure range - which is a good choice for a bladder accumulator - the size of the fixed displacement FC pump can be chosen such, that this pressure range translates to an ICE torque range that runs from 50% to 100% of the ICEs maximum torque. For internal combustion engines, this torque range covers an operation area with very good efficiencies. This way of forcing the ICE to always run in high efficiency points is the crux of the high fuel saving potential of the hydrid concept.

At the secondary side of the driveline, a hydraulic drive unit is connected to each wheel. The two drive units of the front axle are connected to one IHT, the two units of the rear axle to another. The IHTs transform the pressure levels in the CPR to the levels that the fixed displacement wheel motors need in order to realise the required total vehicle drive torque. Details on the IHT and the CPR and their design progression can be found in a large number of Innas publications (for instance [8], [9], [10] and [11]). In the context of this paper, it is sufficient to note that the IHT is continuously variable and that it can transform the pressure in the CPR with very high efficiency, to lower but also to higher output pressure levels.

As has been stated in the introduction, the hydrid driveline is capable of realising the same performance as its conventional counterpart. Therefore, the secondary side of the driveline is sized to meet also the extreme torque requirements. During normal every day driving however, also the secondary part of the driveline will operate in far more moderate conditions. This secondary side gap between the maximum torque available and the average torque needed, implies the risk that the secondary side will mostly operate at lower part load efficiencies. In the hydrid concept, there are three factors that prevent this from happening:

- The use of two separate driving regimes. During normal every day driving, only the wheel motors and IHT of the front axle are engaged and the rear axle system is not. In this way, the torque required from the front axle system is doubled and deep part loads are avoided. This is the first driving regime. In the second driving regime, used only if an extreme torque has to be realised, the rear axle system is also engaged.
- Because of the pressure amplification capability of the IHT, the wheel motors can always be supplied with their maximum pressure (typically 500 bar), even if the CPR pressure is at its lower limit. Without this capability, the wheel motors would have to be big enough to realise the maximum torque at the lowest CPR pressure (typically 200 bar). In that case the wheel motors would have to be chosen a factor 2.5 larger and would – on average – operate deeper in part load by the same factor.
- All hydrostatic units are of the Floating Cup (FC) type, which has superior low speed efficiency. Typically, FC wheel motors have an efficiency of 98% at 350 bar and 0.1 rpm, compared to 75% for the best conventional axial piston units. This implies that FC units can be chosen at least 25% smaller than there conventional counterparts (Background information on the FC principle and its efficiencies, can be found in for instance [12], [13], and [14]).

2.3. The hydrid version of the reference vehicle

The layout chosen for the hydrid version of the reference vehicle is not the same as the original four-wheel drive (4WD) hydrid layout, presented in section 2.2. For this commuter car, a driveline is chosen in which only the front wheels are driven (FWD). Figure 2 shows the system topology.

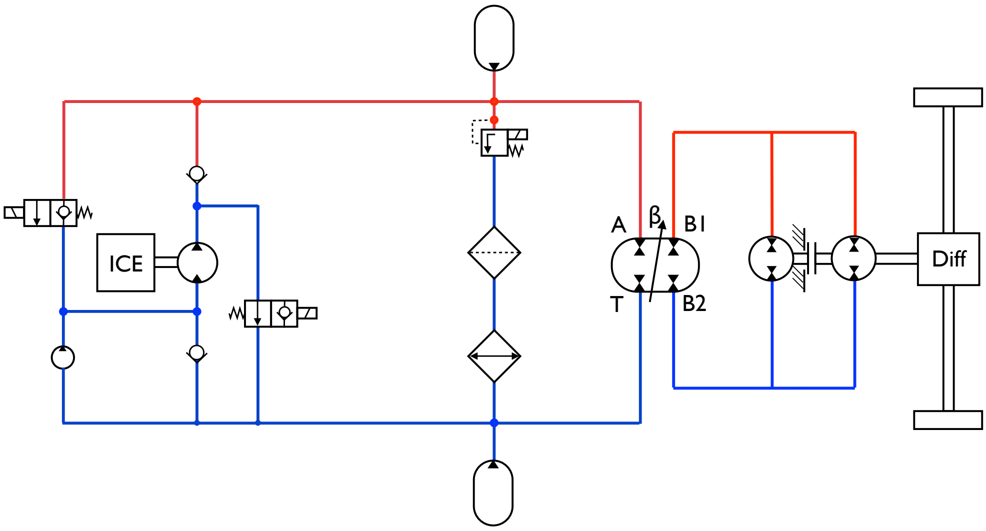

Figure 2. The hydrid driveline for the reference vehicle

In this topology two drive units are connected to the front axle differential: one is permanently connected, the other is piggybacked to the first one and can be engaged or disengaged by means of a double-acting clutch. When the second unit is not engaged, the clutch immobilizes the unit by connecting it to the foundation. In this way the required two drive regimes are realized.

Starting point for the sizing of these two units is the maximum torque requirement for this vehicle. This is predominantly determined by the empty gradeability of the vehicle. For the main vehicle specifications as presented in table 1 and putting the extra weight for the added components of the hydrid driveline to 150 kg, a maximum torque of approximately 1700 Nm is required in order to realise 45% empty gradeability. With a maximum secondary side pressure of 500 bar and the differential ratio of 3.1, the total displacement required for the two drive units together can be calculated to approximately 70 cm^3.

The division of this total swept volume over the two drive units is best illustrated by figure 3. The figure shows the maximum power curve for the ICE, translated to a maximum wheel torque as function of vehicle speed. Obviously, the hydrid system should be able to realise all operating points to the left of this curve. The figure also shows two curves that represent the operational boundaries of the two drive regimes. These two curves can be constructed in the following way:

For any IHT, a pressure transformation curve can be calculated. This curves gives the relationship between the IHTs control angle and its pressure transformation ratio. The form of the curve is a determined only by the IHT's port plate geometry. With this port plate geometry, the IHTs swept volume and its maximum speed a second relationship can be determined. This relationship links the IHTs maximum output flow to its control angle. By combining the two relationships for a given pressure difference between the two lines of the CPR, a relationship between the differential pressure at the IHTs output and its maximum output flow can be derived. With the total swept volume that is coupled to the differential gear in each driving regime, this maximum curve can be mapped to two curves for the maximum drive torque as a function of the maximum vehicle speed.

Figure 3 shows the curves that result if the required 70 cm^3 maximum swept volume is divided over two equally sized drive units, which are driven from a CPR pressure difference of 300 bar, by a 52 cm^3 IHT with a maximum rotational speed of 4000 rpm. With these components, the two regimes cover the maximum power curve of the ICE.

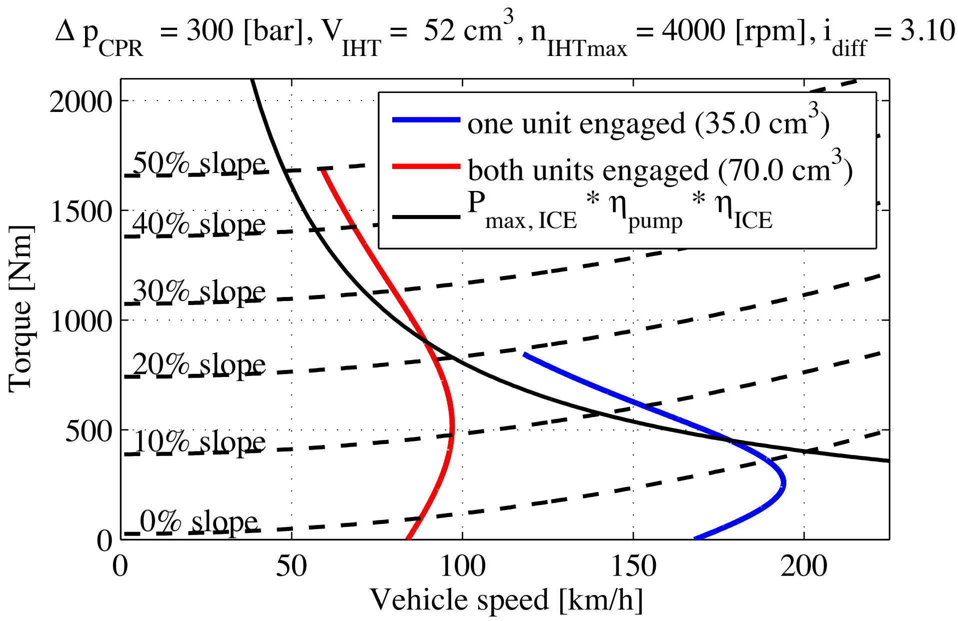

Figure 3. Maximum wheel torque as a function of the vehicle speed.

Figure 3 also shows the maximum wheel torque that the permanently engaged, 35 cm^3 unit can provide. This 800 Nm is more than enough for daily driving, even with a loaded vehicle on the more demanding FTP75 cycle. In other words, with this division of swept volumes, switching to the high torque regime will hardly ever be necessary and the driver will experience a very smooth ride.

The fuel consumption and CO_2-emissions of the resulting hydrid vehicle, when driving the NEDC cycle (the European standard for this purpose), were determined in a so-called 'backward looking' vehicle simulation in Matlab. Table 2 contains the relevant vehicle and driveline data that were used, as well as the resulting fuel consumption and CO_2-emission. The efficiency fields of the used FC units were scaled from measured FC component data, using the techniques described in [15].

This particular hydrid vehicle design realizes a reduction of just over 30% instead of the 50% reduction of the original hydrid concept. This is mostly due to the division of the total swept volume over the two drive units. At the cost of a somewhat more complex system and more switching events, the division could have been made over two units of different size, which can be both engaged or disengaged. In this way, three drive regimes can be realized, and the smallest drive unit runs in significantly better operation points during NEDC circumstances. This alternative has been presented in [16].

Table 2. Specifications and NEDC simulation results of the hydrid vehicle

Specifications			
Engine	Diesel, 80 kW	Differential ratio	3.1
Vehicle weight	1350 kg	FC drive units	35 cm^3 (both)
$r_{tyre, dynamic}$	0.31 m	IHT	52 cm^3
f_{roll}	0.007	FC pump (ICE)	36 cm^3
C_D	0.26	accumulators	15 liter (both)
$A_{frontal}$	2.5 m2	CPR pressure range	200-400 bar
CO_2-emission and fuel consumption on the NEDC			
City	1.8 l/100 km	Combined	3.1 l/100 km
Highway	3.8 l/100 km	CO_2-emission	83 gr/km

Figure 4 shows simulation result for the engine use in this hydrid commuter car and its conventional counterpart. The size of the bubbles in each plot indicates the amount of energy spent near that operating point. The improvement is obvious.

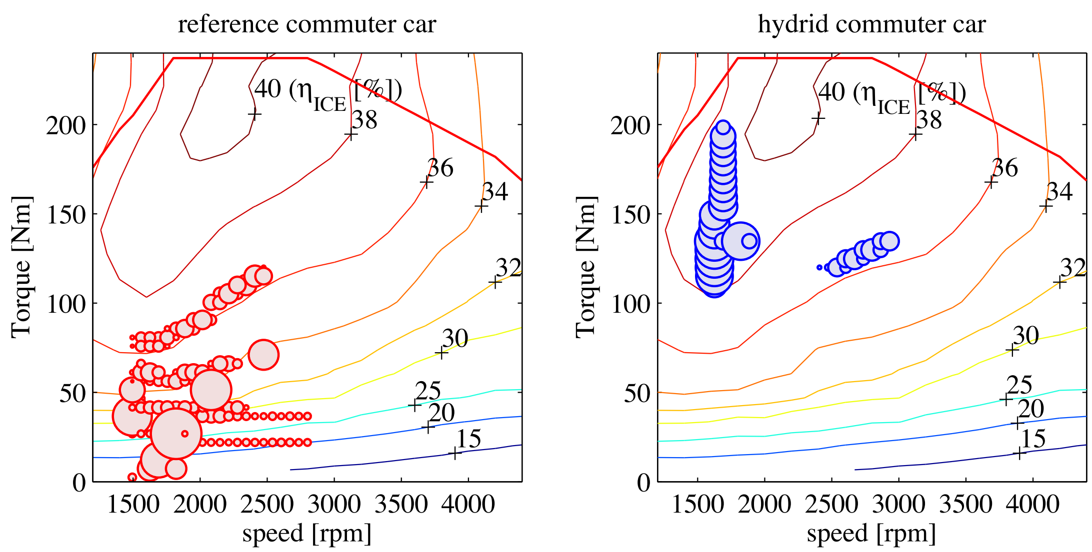

Figure 4. Engine use in the conventional and in the hydrid commuter car.

3. THE E-HYDRID, TOPOLOGY AND SIZING

In the e-hydrid solution, an extra electric energy source is added to the CPR of the hydrid. The energy source consists of a battery, an e-motor that can also act as an electric generator and a FC hydraulic pump that can also act as a hydraulic motor. The resulting driveline topology is shown in figure 5.

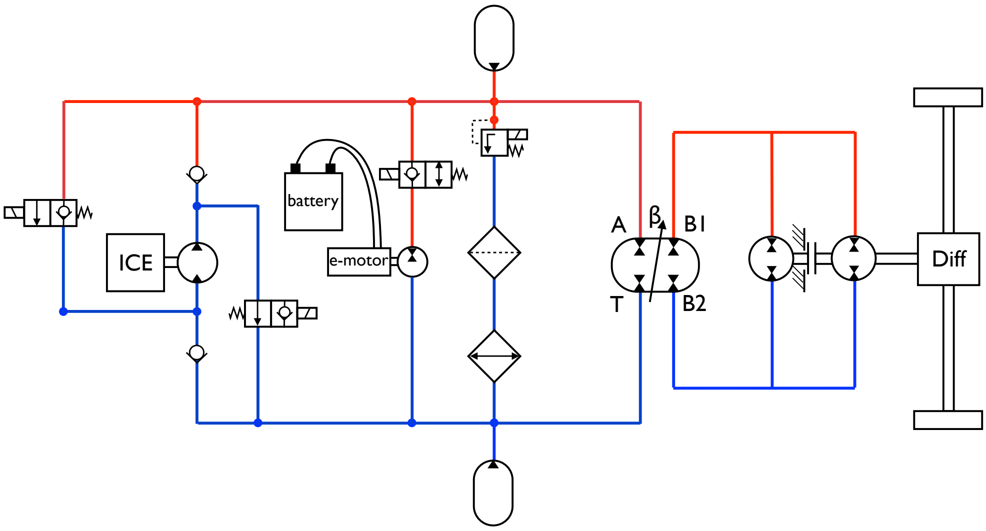

Figure 5. Topology of the e-hydrid

In order to determine the size of the battery, the e-motor and the FC pump, the average energy consumption of this vehicle in urban environments was determined. This was done by simulating the reference hydrid commuter car on both the city part of the NEDC and the city part of the FTP75 cycle. Both cycles are displayed in figure 6; the city parts are marked in red.

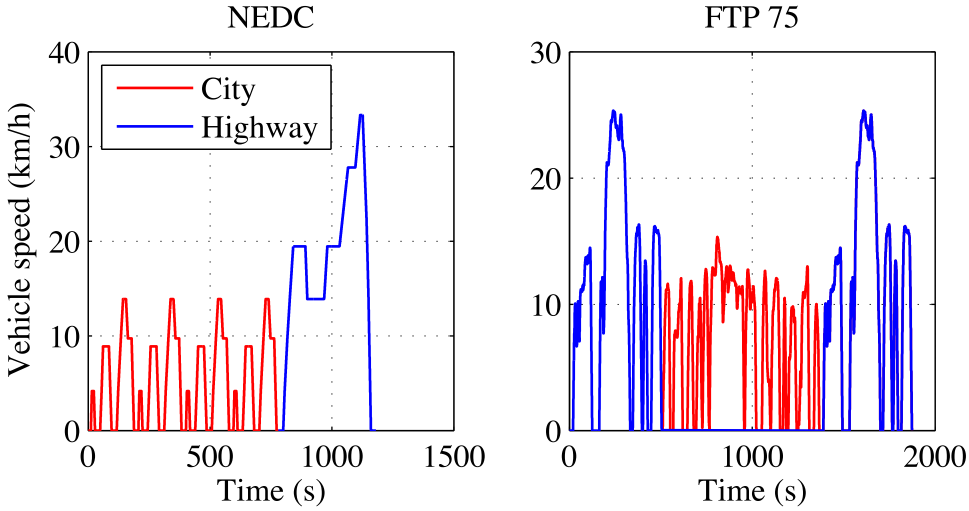

Figure 6. The city part of the NEDC and the FTP75 cycle.

For the simulations on these cycles, the weight of the reference hydrid commuter car was increased with 100 kg, the estimated weight of the added electrohydraulic system. The energy that the FC pump delivers to the CPR on these representative city cycles can be used as an estimate for the energy that the electrohydraulic source has to be able to deliver. Table 3 lists the results as well as some derived parameters.

The table shows that the average electric power required to drive this vehicle in urban areas, is indeed very low: 3.2 kW, assuming that the electric system will only provide power when the vehicle is moving and not when it is standing still.

Table 3. Energy and average power requirements for the electrohydraulic system, on the city part of two representative cycles.

	NEDC		FTP75	
	curb weight	max. loaded	curb weight	max. loaded
Total pump energy [kJ]	1021	1485	1764	2316
Time at nonzero speed [s]	540		717	
Average power [kW]	1.9	2.8	2.5	3.2
Total distance [km]	4.1		6.2	

This average power demand on city cycles is not the only criterion. The electric system should also be able to deliver the continuous power necessary to maintain a sufficient constant speed. For this vehicle, maximally loaded, maintaining a constant speed of around 60 km/h requires 6 kW installed electric power. With this figure, an e-motor was chosen for which a full efficiency map, including the inverter efficiency, was available in literature [17]. This brushless DC-motor is a 42 V, 32-pole Interior Permanent Magnet Synchroneous Machine (IPMSM) unit, with 7 kW continuous power capability, 12 kW intermittent power capability and 40 Nm maximum continuous torque. Its best efficiency area roughly covers a torque range between 20 and 40 Nm and a speed range from 1000 – 2000 rpm. The swept volume of the FC pump should be chosen such that the e-motor is always operated near this sweet spot.

The net battery capacity required for a certain electric range in urban areas can be determined from the simulation results. For the vehicle at curb weight, assuming an efficiency of 85% between battery and CPR, the required battery capacity is approximately 300 kJ/km. This means that for an urban electric range of 20 km, the required range chosen here, the useable battery capacity should be ca. 6 MJ.

Which type of battery is best for this application, is eventually a matter of weight and price. An important factor in this respect is the chosen depth of discharge (DoD) for a certain battery type, as the DoD influences the lifetime of a battery [18], its average cycle efficiency and the maximum battery capacity that has to be installed.

There is a considerable amount of battery data available in literature. Unfortunately, different sources often report data for different battery load collectives and sometimes even contradict each other fundamentally. An additional complication is that the use of the battery in the e-hydrid, is very different from the use in typical electric hybrid vehicle. The e-hydrid battery is not subjected to power peaks – these are dealt with by the hydraulic system – and is discharged with relatively low power. Consequently, this application needs an energy-dense battery more than a power-dense battery.

Initially, a NiMH battery has been chosen for the e-hydrid. In literature an acceptable DoD of 70% and a lowest average discharge efficiency of 85% were found for this kind of battery [19, 20, 21 and 22]. With these values and staying on the safe side, the total capacity required for the NiMH battery for this application was determined to 11.5 MJ. This battery would weigh around 65 kg. Its cells only would typically cost $2000. The lifetime of the battery at this DoD is around 3000 cycles, which corresponds to 60000 urban kilometres. Over the lifecycle, the battery cells would thus cost approximately 0.033 $ per city kilometre.

4. THE E-HYDRID, SIMULATION RESULTS

In order to ensure that the e-motor and battery are used optimally, an appropriate strategy has to be chosen for the state-of-charge (SOC) control of the hydraulic high-pressure accumulator. There are two obvious limits for the SOC as a function of the vehicle speed:

- An upper limit, which ensures that at each vehicle speed up to a certain maximum, there is enough room in the accumulator to recuperate the kinetic energy present in the vehicle.
- A lower limit, which ensures that from each speed, the vehicle can accelerate with an adequate maximum acceleration to a certain maximum speed, without requiring excessive power from the electric system.

The two limit curves that have been adopted in this study are given in figure 7. They have been calculated with the following parameters: vehicle at curb weight, an acceleration capability of 1.5 m/s^2 up to 55 km/h, maximum electric power during an acceleration equal to the maximum continuous power of the chosen e-motor (7 kW).

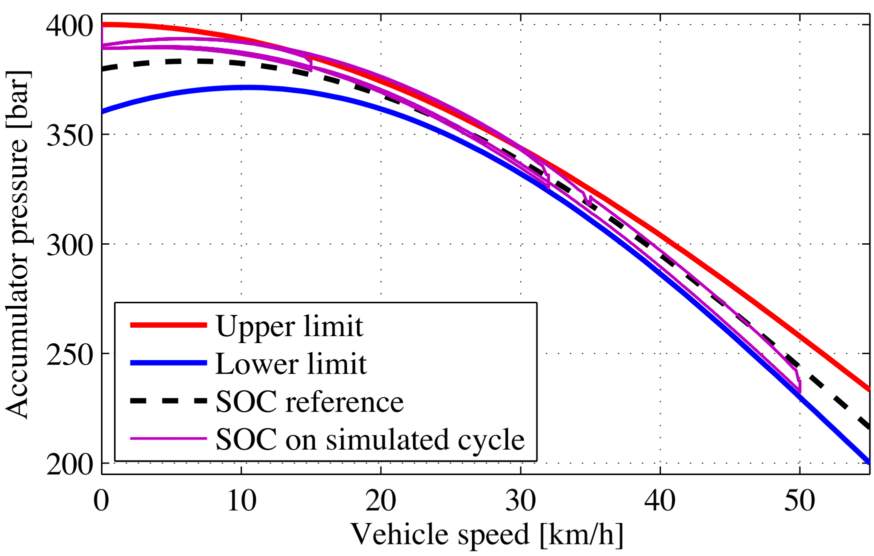

Figure 7. Boundaries and speed reference for the SOC-controller, SOC realization on a simulated NEDC cycle.

For the calculation of these limit curves, aerodynamic vehicle drag and rolling resistance were not taken into account, as they play only a minor role.

The SOC controller in the e-hydrid acts on the e-motor and has to ensure that the accumulator pressure level stays within the two defined limits.

In order to evaluate the performance of the e-hydrid during urban driving, the backward looking simulation model in Matlab was extended with a model of the e-system. The e-motor and FC-pump were modeled using their efficiency maps. The efficiency of the battery was modeled according to [23]. For the SOC control a simple PID-controller was used, which was given the average of the two limit curves as its speed dependent reference curve (See figure 7).

Using the simulation model, a swept volume of 4 cm^3 was determined to be a good choice for the FC pump. Bubbleplots of the use of the e-motor and this FC pump are given in figure 8. Again, the size of the bubbles indicates the amount of energy spent at that operating point. The plots show that – for this FC pump size and with this controller strategy – both the e-motor and the FC pump operate at very good average efficiencies.

The plot also shows that the power required from the e-system indeed represents a very friendly battery-load. The battery model predicts an average battery efficiency of 95.6% for this load collective.

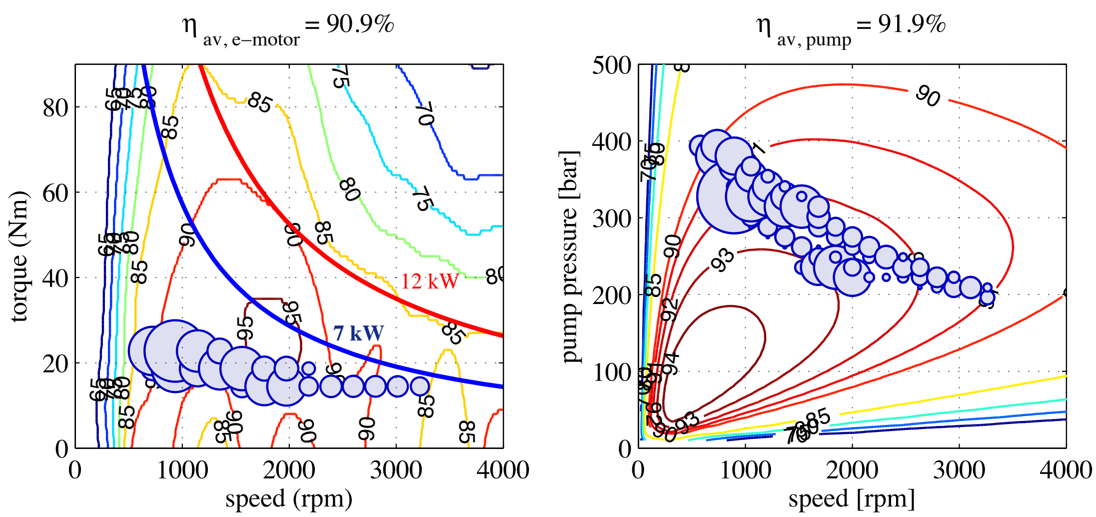

Figure 8. Use of the e-motor and the FC pump

Over the 4.1 km NEDC city drive, the energy taken from the battery was 1.3 MJ. For the installed total battery capacity of 11.5 MJ and 70% DoD, this implies an all-electric range of 25 km when driving the city part of the NEDC cycle.

The SOC over the simulated cycle, as a function of the vehicle speed, is also given in figure 7. It shows that the SOC controller performs adequately.

5. CONCLUSION AND OUTLOOK

The e-hydrid commuter car, presented in this paper, offers a 25 km all-electric range on urban drive cycles, with only a very small electric add-on system. Due to the hydraulic backbone system the e-hydrid meets all of the performance characteristics of the reference car it is based on (which in this case is a quite potent car), at least on flat roads. On inclined roads and driving on the e-system alone, the maximum speed on the slope is limited by the installed maximum e-power (12 kW in this case). In other words, in e-mode, the e-hydrid can negotiate any slope up to the maximum (45% in this case); the only drawback is that its maximum speed is grade-dependant. In a similar way, the height difference that can be negotiated in e-mode is limited by the battery capacity. For this design it is approximately 300 meter.

When electric driving is not compulsory or when the battery is empty after a daily drive into an urban, e-only area, the system can function on the ICE with exactly the same advantages as the original hydrid concept: all performance characteristics are on par with the conventional reference vehicle and the fuel consumption and CO_2 emissions on representative cycles are reduced with more than 30% (83 grams of CO_2 on the NEDC).

The system offers an option for the recharging of the battery:

- It can be charged from the ICE over the CPR, when driving to or from an e-only area. The charging events can be used to bring the ICE in operating points of better efficiency, thus increasing the average engine efficiency even further.
- It can be charged from the electricity grid, if a suitable charging point is available.

The decision can be made for economic or logistic reasons. Plug-in charging is cheaper and slightly better in terms of CO_2 emissions (assuming the West-European electricity production mix) but where charging infrastructure is sparse, the vehicle can operate autonomously with all consumption and emission advantages of the standard hydrid.

The e-hydrid driveline concept is very flexible. The division of the installed primary power between the internal combustion engine and the electric system can be changed according to the design goals. For this study, the goal was to minimise the size of the electric side of the system, in order to minimise the vehicle costs. If however, political choices or technological advances act in favour of electric components, it is very easy to install more electrical and less ICE power, even up to the point that the vehicle becomes an all-electric vehicle or an electric vehicle with an ICE as a range-extender. The CPR enables easy integration of any power source and provides the peak shaving capacity that is beneficial for all electric solutions.

Increasing the battery capacity and/or the e-motor power is a possible solution if the speed dependant gradeability and/or the maximum height difference, are considered too limiting for cities with a pronouncedly hilly character. But even for those cities, a larger reduction of local emission can be reached with a large fleet of cheaper e-hydrids, which are allowed to occasionally use their ICE within the city, instead of a small fleet of more expensive conventional plug-in electric hybrid vehicles.

REFERENCES

1 Peter Achten, Georges Vael, Torsten Kohmäscher, Mohammed Sokar, *Energy Efficiency of the Hydrid,* 6th Int. Fluid Power Conf., Dresden, 2008.

2 Peter Achten, Georges Vael, Hubertus Murrenhoff, Torsten Kohmäscher, Martin Inderelst. *Low-emission Hydraulic Hybrid for Passenger Cars*, ATZ, Vol. 111, May 2009.

3 The Boston Consulting Group (BCG), *Batteries for Electric Cars – Challenges, Opportunities and the Outlook to 2020,* BCG Focus, 2010.

4 William Tahil, *The Trouble with Lithium – Implication of Future PHEV Production for Lithium Demand,* Meridian International Research, 2006.

5 *Kosten und Potenziale der Vermeidung von Treibhausgasemissionen in Deutschland*, McKinsey and Company, September 2007.

6 *Pathways to a Low-Carbon Economy - Version 2 of the Global Greenhouse Gas Abatement Cost Curve*, McKinsey and Company, September 2009.

7 Menahem Anderman, *Status and Prospects of Battery Technology for Hybrid Electric Vehicles, Including Plug-in Hybrid Electric Vehicles*, Briefing to the U.S. Senate Committee on Energy and Natural Resources, Advanced Automotive Batteries, 2007.

8 Peter A.J. Achten PhD, Zhao Fu PhD, Georges E.M. Vael, *Transforming future hydraulics: a new design of a hydraulic transformer,* The Fifth Scandinavian International Conference on Fluid Power, SICFP '97, 1997, Linköping, Sweden.

9 G. E. M. Vael, P. A. J. Achten, and Z. Fu, *The Innas Hydraulic Transformer - the Key to the Common Pressure Rail*, SAE International Off-Highway and Powerplant Congress and Exhibition, no. 2000-01- 2561, Society of Automotive Engineers (SAE), September 2000.

10 G.E.M. Vael, T.L. van den Brink, T. Paardenkooper, P.A.J. Achten, *Some Design Aspects of the Floating Cup Hydraulic Transformer*,

11 P. Achten, T. van den Brink, J. Potma, M. Schellekens, and G. Vael, *A four-quadrant hydraulic transformer for hybrid vehicles*, The 11th Scandinavian International Conference on Fluid Power, SICFP'09, 2009, Linköping, Sweden.

12 P. Achten, T. van den Brink, T. Paardenkooper, T. Platzer, J. Potma, M. Schellekens, and G. Vael, *Design and testing of an axial piston pump based on the floating cup principle,* The Eighth Scandinavian international Conference on Fluid Power (SICFP'03), Tampere, May 2003.

13 Dr.ir. W. Post, *Determination of the steady-state performance of a 28 [cm3] Innas Variable Floating Cup Pump (FCV28)*, CST Report 2010.011, Eindhoven University of Technology, Department of Mechanical Engineering, Control Systems Technology Group, March 2010

14 Peter Achten, Georges Vael, Titus van den Brink, Jeroen Potma, Marc Schellekens, *Efficiency Measurements of the Hydrid Motor/Pump*, The Twelfth Scandinavian International Conference on Fluid Power, SICFP'11, May 18-20, 2011, Tampere, Finland

15 Georges E.M. Vael, Peter A.J. Achten and Titus van den Brink, *Efficiency of a Variable Displacement Open Circuit Floating Cup Pump*, The 11th Scandinavian International Conference on Fluid Power, SICFP'09, 2009, Linköping, Sweden.

16 Georges Vael, Peter Achten (2010). *IHT controlled serial hydraulic hybrid passenger cars*, 7th Int. Fluid Power Conference, 2010, Aachen, Germany.

17 Jonas Ottosson, *Energy Management and Control of Electrical Drives in Hybrid Electrical Vehicles*, Licentiate Thesis, Lund University, Department of Industrial Electrical Engineering and Automation, 2007.

18 Lorenzo Serrao, Zakaria Chehab, Yann Guezennec and Giorgio Rizoni, *An Aging Model of Ni-MH Batteries for Hybrid Electric Vehicles*, The Ohio State University, Center for Automotive Research, 2005 IEEE, Columbus, USA.

19 Sheldon Williamson, *Electric Drive Train Efficiency Analysis Based on Varied Energy Storage System Usage for Plug-In Hybrid Electric Vehicle Applications*, Concordia University, Department of Electrical and Computer Engineering, P.D. Ziogas Power Electronics Laboratory, 2007 IEEE, Quebec, Canada.

20 Jens Tübke, Thomas Berger, Thomas Bayha, Matthias Krampfert, *Elektrochemische Energiespeicher in mobile Anwendungen*, Hybridantriebe für mobile Arbeitsmaschinen, 2. Fachtagung des VDMA und der Unversität Karlsruhe (TH), Februar 2009, Karlsruhe, Deutschland.

21 I. Menjak, P.H. Gow, D.A. Corrigan, S. Venkatesan, S.K. Dhar, R.C. Stempel and S.R. Ovshinsky, *Advanced Ovonic High-Power Nickel-Metal Hydride Batteries for Hybrid Electric Vehicle Applications*, Ovonic Battery Company, 1998 IEEE, Troy, Michigan, USA

22 W.H. DeLuca, A.F. Tummillo, J.E. Kulaga, C.E. Webster, K.R. Gillie and R.L. Hogrefe, *Performance Evaluation of Advanced Battery technologies for Electric Vehicle Applications*, Argonne National Laboratory, 1990, Illinois, USA.

23 Olivier Tremblay, Louis-A. Dessaint and Abdel-Illah Dekkiche, *A Generic Battery Model for the Dynamic Simulation of Hybrid Electric Vehicles*, Universite du Quebec, Ecole de Technologie Superieure, Groupe de Recherche en Electronique de Puissance et Commande Industrielle (GREPCI), 2007 IEEE, Quebec, Canada.